

## **Extracts of the 2006 Annual Report of the (former) JGU “Institute of Nuclear Chemistry”**

### **Search for the “Missing” $\alpha$ -Decay Branch in $^{239}\text{Cm}$**

**Page 2**

Z. Quin, D. Ackermann, W. Bröchle, F. P. Hessberger, E. Jäger, P. Kuusiniemi, G. Münzenberg, D. Nayak, E. Schimpf, M. Schädel, B. Schausten, A. Semchenkov, B. Sulignano, X. L. Wu, K. Eberhardt, J. V. Kratz, D. Liebe, P. Thörle, Yu. N. Novikov

### **TASCA Recoil Transfer Chamber Commissioning. 1. Small Image Mode**

**Page 3**

Ch. E. Düllmann, D. Ackermann, W. Bröchle, F.P. Heßberger, E. Jäger, J. Khuyagbaatar, M. Schädel, B. Schausten, E. Schimpf, H.-J. Schött, A. Semchenkov, J. Dvorak, A. Gorshkov, R. Schuber, A. Türler, A. Yakushev, K. Eberhardt, H. Hummrich, J. V. Kratz, J. P. Omtvedt, K. Opel, J.M. Gates, K.E. Gregorich, R. Dressler, R. Eichler, Z. Gan

### **TASCA Recoil Transfer Chamber Commissioning. 2. High Transmission Mode**

**Page 4**

Ch. E. Düllmann, D. Ackermann, W. Bröchle, F.P. Heßberger, E. Jäger, J. Khuyagbaatar, M. Schädel, B. Schausten, E. Schimpf, H.-J. Schött, A. Semchenkov, J. Dvorak, A. Gorshkov, R. Schuber, A. Türler, A. Yakushev, K. Eberhardt, H. Hummrich, J. V. Kratz, J. P. Omtvedt, K. Opel, J.M. Gates, K.E. Gregorich, R. Dressler, R. Eichler, Z. Gan

### **Window Design for the TASCA Recoil Transfer Chamber (RTC)**

**Page 5**

A. Yakushev, A. Semchenkov, J. Dvorak, A. Türler, D. Ackermann, W. Bröchle, Ch. E. Düllmann, E. Jäger, M. Schädel, B. Schausten, E. Schimpf, H. Hummrich, J. V. Kratz, K.E. Gregorich, J.P. Omtvedt, K. Opel, R. Eichler

### **Target Development for TASCA**

**Page 6**

K. Eberhardt, J.V. Kratz, D. Liebe, P. Thörle, W. Bröchle, Ch. E. Düllmann, W. Hartmann, A. Hübner, E. Jäger, B. Kindler, B. Lommel, M. Schädel, B. Schausten, E. Schimpf, A. Semchenkov, J. Steiner, K.E. Gregorich, H.-J. Maier, J. Szerypo, R. Sudowe, A. Türler, A. Yakushev

### **Improvements at the radiographic analysis of radioactive targets**

**Page 7**

D. Liebe, K. Eberhardt, J.V. Kratz, W. Hartmann, A. Huebner, B. Kindler, B. Lommel, J. Steiner

### **Fast electrochemical deposition of Bismuth**

**Page 8**

H. Hummrich, J.V. Kratz

# Search for the "Missing" $\alpha$ -Decay Branch in $^{239}\text{Cm}$

Z. Qin<sup>1,3</sup>, D. Ackermann<sup>1</sup>, W. Bröchle<sup>1</sup>, F.P. Hessberger<sup>1</sup>, E. Jäger<sup>1</sup>, P. Kuusiniemi<sup>1</sup>,  
G. Münzenberg<sup>1</sup>, D. Nayak<sup>1</sup>, E. Schimpf<sup>1</sup>, M. Schädel<sup>1</sup>, B. Schausten<sup>1</sup>, A. Semchenkov<sup>1</sup>  
B. Sulignano<sup>1,2</sup>, X.L. Wu<sup>1,3</sup>, K. Eberhardt<sup>2</sup>, J.V. Kratz<sup>2</sup>, D. Liebe<sup>2</sup>, P. Thörle<sup>2</sup>, Yu. N. Novikov<sup>1,4</sup>

<sup>1</sup>GSI, Darmstadt, Germany, <sup>2</sup>Johannes Gutenberg-Universität, Mainz, Germany,  
<sup>3</sup>IMP, Lanzhou, P.R. China, <sup>4</sup>Petersburg Nuclear Physics Institute, Gatchina, Russia

Our first series of experiments yielded an upper limit of  $3 \times 10^{-5}$  for the  $\alpha$ -decay branch of  $^{239}\text{Cm}$  [1,2] produced in the  $^{12}\text{C} + ^{232}\text{Th}$  reaction. In these experiments only  $\alpha$ -spectra were evaluated as the  $\gamma$ -spectra were not clean enough to identify  $\gamma$ -lines from the decay of  $^{239}\text{Cm}$  or its daughter  $^{239}\text{Am}$ . Due to the use of 3.9  $\mu\text{m}$  thick Cu catcher foils in a rotating catcher wheel behind a rotating target setup  $\gamma$ -spectra dominantly showed lines from the decay of  $^{153}\text{Sm}$ ,  $^{150,151}\text{Pm}$ , and  $^{147,149}\text{Nd}$ . Those homologous rare earth elements, produced in fission with cross sections of about 5 mb, were stopped in the Cu catcher but were only partly separated in the chemical procedure.  $^{71,72}\text{As}$  and  $^{69}\text{Ge}$ , produced in reactions of  $^{12}\text{C}$  with the Cu catcher, created an additional background.

In recent experiments 1  $\mu\text{m}$  thick Cu foils produced by the GSI target laboratory were used in 120-150 mbar He in stationary target-catcher setups. These foils are sufficiently thick to stop all fusion products (0.3  $\mu\text{m}$  range) but thin enough to let most fission products pass (3-6  $\mu\text{m}$  range) and to minimize interaction of the  $^{12}\text{C}$  beam with the Cu catcher. This provided a breakthrough and allowed identifying the 188 keV  $\gamma$ -line assigned to  $^{239}\text{Cm}$  [3] as well as  $\gamma$ -lines of the EC-decay daughter  $^{239}\text{Am}$ .  $^{239}\text{Cm}$  was produced in ( $\leq 0.4 \mu\text{A}_{\text{part}}$ )  $^{12}\text{C} + ^{232}\text{Th}$  reactions. A faster and more efficient chemical separation procedure was applied [4]. Instead of two different elution media with 0.25M and 0.30M  $\alpha$ -HIB the whole separation was conducted with 0.40M  $\alpha$ -HIB at pH=4.6. Figure 1 shows improved elution curves from a cation exchange resin. Since this time all samples contained only small amounts of Sm and Pm, we added  $^{244}\text{Cm}$  as a tracer making the yield determination even more reliable. Overall yields varied between 75% and 90%.

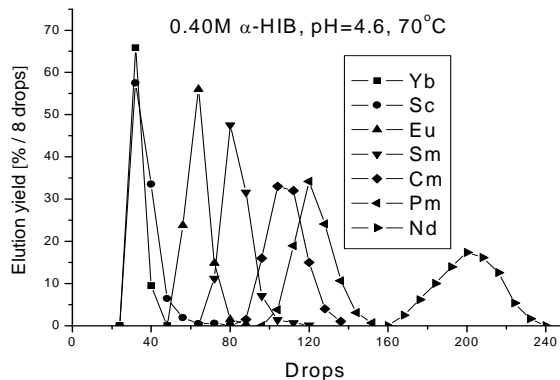


Figure 1: Chromatogram with tracer elements. Drops 80 to 150 were selected as the Cm fraction.

We performed irradiations at 74, 70 and 66 MeV  $^{12}\text{C}$  energies in the middle of the 360  $\mu\text{g}/\text{cm}^2$  Th targets. 74 MeV was selected because at this energy HIVAP calculations predict the highest  $^{239}\text{Cm}$  cross section. However, as we cannot exclude that  $\alpha$ -events observed around 6.4 MeV stem from tailing of the 6.52 MeV  $\alpha$ -lines of  $^{238}\text{Cm}$ , which is abundantly produced at this energy and which has a similar half-life, no attempt was made to determine an  $\alpha$ -decay branch in  $^{239}\text{Cm}$  from this experiment.

70 MeV was selected because interfering  $^{238}\text{Cm}$  should be produced less by a factor of 80, whereas production of  $^{239}\text{Cm}$  should drop by a factor of 1.7 only. Finally, 66 MeV was chosen because  $^{240}\text{Cm}$  has its production maximum there. This allowed to check if events around 6.4 MeV can be produced by  $\alpha$ - $\beta$ -pileup. Though the  $^{240}\text{Cm}$  activity was higher than in the other experiments, not a single  $\alpha$  could be detected between 6.35 and 7.0 MeV during the first day of measuring time. The 188 keV  $\gamma$ -line, assigned to  $^{239}\text{Cm}$  [3], was measured in experiments at 70 and 74 MeV irradiation energy. In addition, the 229 and 278 keV  $\gamma$ -lines of the daughter product  $^{239}\text{Am}$  were detected. Since at 70 MeV irradiation energy HIVAP predicts a factor of 2000 lower cross section for  $^{239}\text{Am}$  as compared to  $^{239}\text{Cm}$ , we feel safe to attribute all measured  $^{239}\text{Am}$  to  $^{239}\text{Cm}$  daughters. As the absolute intensity of the  $^{239}\text{Cm}$  188 keV  $\gamma$ -line is not known, we started our analysis with the assumption of 100% abundance. Based on this we calculated how much  $^{239}\text{Am}$  is produced in the  $^{239}\text{Cm}$  EC-decay. As the experimentally observed amount of  $^{239}\text{Am}$  at 70 MeV is a factor of  $2.8 \pm 0.8$  higher, we concluded that the 188 keV  $\gamma$ -line has an intensity of about 36%. The error (90% c.i.) includes uncertainties in the half-life of  $^{239}\text{Cm}$  between 2 and 4 h and in the Cm-Am separation yield between 30% and 70%. The 70 MeV experiments yielded five  $\alpha$ -decays between 6.36 and 6.45 MeV within the first 10 h of measurement. An average background of 0.625 events, determined in a long background measurement without a sample, was subtracted (note that the background with a sample could be somewhat higher). This yields a ratio of  $\alpha$ -decay to EC decay of  $\leq 1.9 \times 10^{-5}$  (90% c.i.) and  $\leq 1.4 \times 10^{-5}$  (68.3% c.i.) for the decay of  $^{239}\text{Cm}$ .

## References

- [1] Z. Qin et al., GSI Scientific Report 2004, p.190
- [2] Z. Qin et al., GSI Scientific Report 2005, p.197
- [3] E. Browne, Nucl. Data Sheets 98, 665 (2003).
- [4] Z. Qin et al., GSI Scientific Report 2004, p.191.

## TASCA Recoil Transfer Chamber Commissioning. 1. Small Image Mode

Ch.E. Düllmann<sup>1,\*</sup>, D. Ackermann<sup>1</sup>, W. Bröchle<sup>1</sup>, F.P. Heßberger<sup>1</sup>, E. Jäger<sup>1</sup>, J. Khuyagbaatar<sup>1</sup>, M. Schädel<sup>1</sup>, B. Schausten<sup>1</sup>, E. Schimpf<sup>1</sup>, H.-J. Schött<sup>1</sup>, A. Semchenkov<sup>1,2</sup>, J. Dvorak<sup>2</sup>, A. Gorshkov<sup>2</sup>, R. Schuber<sup>2</sup>, A. Türler<sup>2</sup>, A. Yakushev<sup>2</sup>, K. Eberhardt<sup>3</sup>, H. Hummrich<sup>3</sup>, J.V. Kratz<sup>3</sup>, J.P. Omtvedt<sup>4</sup>, K. Opel<sup>4</sup>, J.M. Gates<sup>5,6</sup>, K.E. Gregorich<sup>5</sup>, R. Dressler<sup>7</sup>, R. Eichler<sup>7,8</sup>, Z. Gan<sup>9</sup>

<sup>1</sup>GSI, Darmstadt, Germany; <sup>2</sup>TU Munich, Garching, Germany; <sup>3</sup>U Mainz, Germany; <sup>4</sup>U Oslo, Norway; <sup>5</sup>LBL, Berkeley, CA, USA; <sup>6</sup>UC Berkeley, CA, USA; <sup>7</sup>PSI, Villigen, Switzerland; <sup>8</sup>U Berne, Switzerland; <sup>9</sup>IMP Lanzhou, P.R. China.

One of the main foreseen applications of the gas-filled TransActinide Separator and Chemistry Apparatus (TASCA) [1] recently installed at GSI is its use as a physical preseparator for chemistry experiments [2,3] see configuration shown in Figure 1. As has been described before [4,5] two different ion optical modes are available at TASCA. For both TASCA modes, the Small Image Mode (SIM) as well as the High Transmission Mode (HTM), Recoil Transfer Chambers (RTC) that match the focal plane images and corresponding flanges accommodating the RTC windows [5] have been built. In this report, commissioning of the SIM RTC built at the University of Oslo is described while the commissioning experiments with the HTM RTC can be found in [6].

The SIM leads to an image size of  $\sim(30 \times 40)$  mm<sup>2</sup> in the focal plane. Correspondingly, an RTC attached to TASCA in this mode can be constructed with a very small volume. This is advantageous for studies of relatively short-lived species with half-lives of only a few seconds or even less, as decay losses occurring during flushing out of the RTC are minimal.

Construction of the interface between TASCA and the RTC, the RTC window and its support structure is described in [5]. The inner diameter of the SIM RTC is only 30 mm, leading to a very small volume compared to RTCs in operation at BGS/LBNL [2], GARIS/RIKEN [8] or the TASCA HTM RTC [6]. The SIM RTC is built in a modular way. Thus, its depth and the gas flow configuration can be changed. Using different spacers allows adopting depths between 10 and 57 mm with the gas entry position to be chosen freely between 5 mm and 22 mm behind the RTC window.

The SIM RTC was commissioned with short-lived Hg isotopes produced in the  $^{144}\text{Sm}(^{40}\text{Ar},\text{xn})^{184-\text{x}}\text{Hg}$  reaction. Preseparated Hg atoms were thermalized in a 30 mm deep RTC and transported with a pure He gas flow (2.0 l/min) through a  $\sim 13$  m long PTFE capillary (i.d. 2.0 mm) to the detection system. The Cryo On-line Multidetector for Physics And Chemistry of Transactinides (COMPACT) [8] was used. It consisted of an array of 32 pairs of Au covered PIPS detectors forming a narrow channel. Hg is known to adsorb on Au surfaces [9]. COMPACT was operated in the isothermal regime at room temperature. The obtained  $\alpha$ -spectrum (Figure 2) clearly shows the high separation quality of TASCA in combination with the employed chemical separation system consisting of a pure He jet and COMPACT. Only lines of Hg isotopes and their daughters are visible.

\*c.e.duellmann@gsi.de

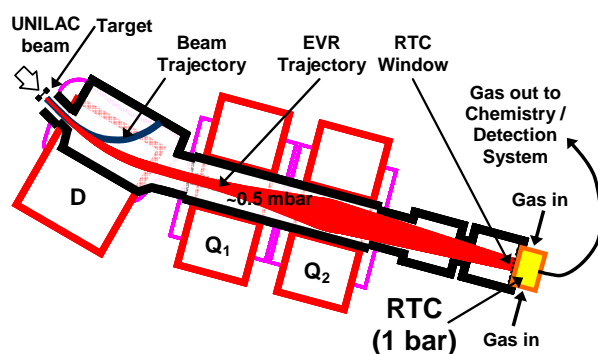


Figure 1: TASCA in the preseparator configuration

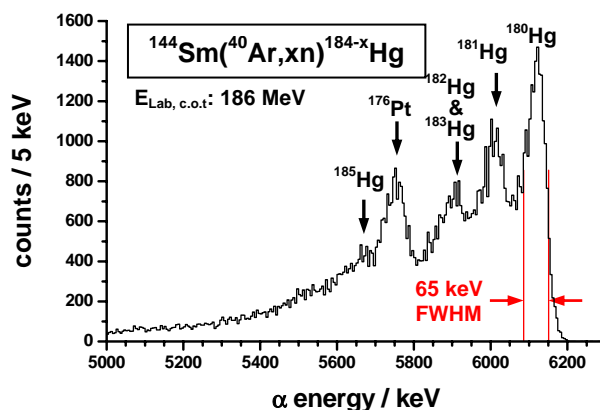


Figure 2:  $\alpha$ -spectrum measured with COMPACT [8].

### References

- [1] M. Schädel *et al.*, GSI Sci. Rep. 2005, Report 2006-1, 2006, p. 262; see also <http://www.gsi.de/TASCA>.
- [2] Ch.E. Düllmann *et al.*, Nucl. Instrum. Meth. **A551** (2005) 528.
- [3] J.P. Omtvedt *et al.*, J. Nucl. Radiochem. Sci. **3** (2002) 121.
- [4] A. Semchenkov *et al.*, GSI Sci. Rep. 2004, Report 2005-1, p. 332.
- [5] A. Yakushev *et al.*, contribution to this report.
- [6] Ch.E. Düllmann *et al.*, contribution to this report.
- [7] H. Haba, private communication.
- [8] J. Dvorak *et al.*, GSI Sci. Rep. 2004, Report 2005-1, p. 183.
- [9] S. Soverna *et al.*, Radiochim. Acta **93** (2005) 1.

Acknowledgements: Thanks to Inge Mikalsen at the University of Oslo who built the SIM RTC in record time.

## TASCA Recoil Transfer Chamber Commissioning. 2. High Transmission Mode

Ch.E. Düllmann<sup>1,\*</sup>, D. Ackermann<sup>1</sup>, W. Bröchle<sup>1</sup>, F.P. Heßberger<sup>1</sup>, E. Jäger<sup>1</sup>, J. Khuyagbaatar<sup>1</sup>, M. Schädel<sup>1</sup>, B. Schausten<sup>1</sup>, E. Schimpf<sup>1</sup>, H.-J. Schött<sup>1</sup>, A. Semchenkov<sup>1,2</sup>, J. Dvorak<sup>2</sup>, A. Gorshkov<sup>2</sup>, R. Schuber<sup>2</sup>, A. Türler<sup>2</sup>, A. Yakushev<sup>2</sup>, K. Eberhardt<sup>3</sup>, H. Hummrich<sup>3</sup>, J.V. Kratz<sup>3</sup>, J.P. Omtvedt<sup>4</sup>, K. Opel<sup>4</sup>, J.M. Gates<sup>5,6</sup>, K.E. Gregorich<sup>5</sup>, R. Dressler<sup>7</sup>, R. Eichler<sup>7,8</sup>, Z. Gan<sup>9</sup>

<sup>1</sup>GSI, Darmstadt, Germany; <sup>2</sup>TU Munich, Garching, Germany; <sup>3</sup>U Mainz, Germany; <sup>4</sup>U Oslo, Norway; <sup>5</sup>LBL, Berkeley, CA, USA; <sup>6</sup>UC Berkeley, CA, USA; <sup>7</sup>PSI, Villigen, Switzerland; <sup>8</sup>U Berne, Switzerland; <sup>9</sup>IMP Lanzhou, P.R. China.

The TASCA separator [1] has entered the phase where the different components are commissioned in dedicated experiments. In 2006, two of those components were the Recoil Transfer Chambers (RTCs) [2] that transfer the species separated in TASCA to a chemistry setup. While the RTC designed for the Small Image Mode (SIM) [3] of TASCA is described in [4], the one constructed for the High Transmission Mode (HTM) [3] is described here.

In the highly efficient HTM configuration, EVaporation Residues (EVRs) are guided into an area of  $\sim(140 \times 40)$  mm<sup>2</sup> in the focal plane. The HTM RTC (Figure 1) was built at the University of Mainz. It features a modular arrangement that allows easy change of its depth and gas flow pattern. Eight connections are located around the RTC, allowing the investigation of the flushing-out efficiency for different gas flow modes. A catcher foil can be mounted in a position close to the RTC window, thus allowing to measure the activity entering the RTC. The RTC window (140x40 mm<sup>2</sup> area) that separates TASCA's low pressure regime from the high pressure in the RTC was designed and built at the TU Munich, Garching [5].

In the reaction  ${}^{\text{nat}}\text{Gd}({}^{40}\text{Ar}, \text{xn})^{-194}\text{Pb}$ , relatively long-lived Pb isotopes were produced and thermalized in a 35-mm deep RTC. A He/KCl gas-jet (1.1 l/min) was used to transport pre-separated EVRs through a  $\sim 13$  m long PTFE capillary (i.d. 1.5 mm) to a radiochemical laboratory. Two different configurations were used: in the first one (configuration as displayed by black arrows in Figure 1), the gas entered the RTC through six gas inlets located around the RTC and left the RTC through the center of the cover. In the second one (Figure 1, light arrows), the gas was swept across the RTC window by entering through three inlets on the left side and leaving through three exits on the right side. Aerosol particles were collected on a glass fiber filter that was placed in front of a low energy photon counter for  $\gamma$  counting.

An unexpectedly low gas-jet yield of only  $\sim 15\%$  was measured for both gas flow modes. This could be due to a low particle density or indicate that Teflon is not a suitable tubing material for use with particle gas-jets. Figure 2 shows a  $\gamma$  spectrum taken in these studies. It was obtained by measuring a filter containing pre-separated EVRs from a 10 min long irradiation. Acquisition was started five min after the end of bombardment; the counting time was five min. Only  $\gamma$  lines of Pb isotopes and their daughters are visible, proving that all unwanted reaction products are strongly suppressed. This is in contrast

to studies with non-pre-separated Pb isotopes [6] where dominating  $\gamma$  lines originated from unwanted isotopes such as  ${}^{49}\text{Cr}$  or  ${}^{43\text{m},44}\text{Sc}$  produced in reactions of the beam with various parts of the target setup.

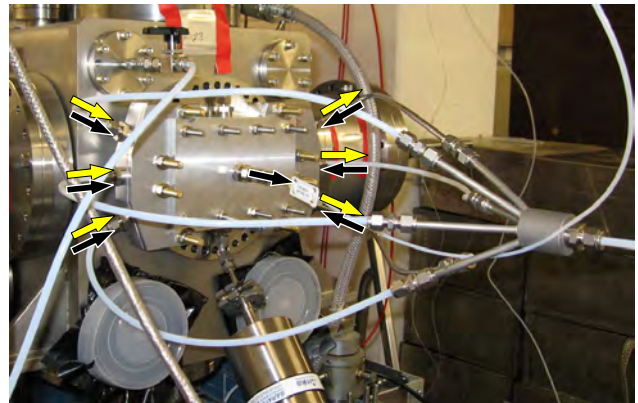


Figure 1: The HTM RTC mounted at TASCA. The two gas flow regimes are indicated by light and dark arrows.

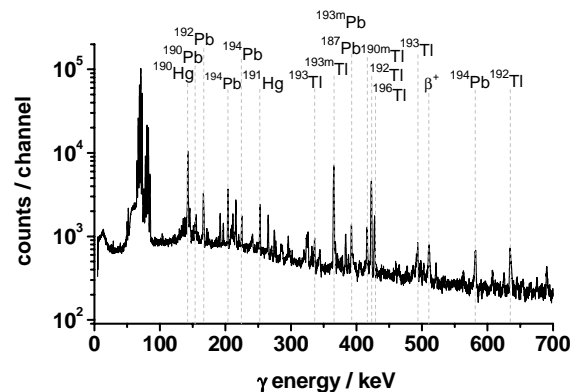


Figure 2:  $\gamma$  spectrum obtained in the commissioning run.

### References

- [1] M. Schädel *et al.*, GSI Sci. Rep. 2005, Report 2006-1, 2006, p. 262; see also <http://www.gsi.de/TASCA>.
- [2] Ch.E. Düllmann *et al.*, Nucl. Instrum. Meth. **A551** (2005) 528.
- [3] A. Semchenkov *et al.*, GSI Sci. Rep. 2004, Report 2005-1, p. 332.
- [4] Ch.E. Düllmann *et al.*, contribution to this report.
- [5] A. Yakushev *et al.*, contribution to this report.
- [6] H. Hummrich, Doctoral thesis, U Mainz, 2006.

Acknowledgements: Thanks to the mechanical workshop staff at Mainz University for the fast building of the RTC.

\* c.e.duellmann@gsi.de

## Window Design for the TASCA Recoil Transfer Chamber (RTC)

A. Yakushev<sup>1,\*</sup>, J. Dvorak<sup>1</sup>, A. Semchenkov<sup>1,2</sup>, A. Türler<sup>1</sup>, D. Ackermann<sup>2</sup>, W. Brüchle<sup>2</sup>, Ch.E. Düllmann<sup>2</sup>, E. Jäger<sup>2</sup>, M. Schädel<sup>2</sup>, B. Schausten<sup>2</sup>, E. Schimpf<sup>2</sup>, H. Hummrich<sup>3</sup>, J.V. Kratz<sup>3</sup>, K.E. Gregorich<sup>4</sup>, J.P. Omtvedt<sup>5</sup>, K. Opel<sup>5</sup>, R. Eichler<sup>6,7</sup>

<sup>1</sup>TU Munich, Garching, Germany; <sup>2</sup>GSI, Darmstadt, Germany; <sup>3</sup>U Mainz, Germany; <sup>4</sup>LBNL, Berkeley, CA, USA; <sup>5</sup>U Oslo, Norway; <sup>6</sup>PSI, Villigen, Switzerland; <sup>7</sup>U Berne, Switzerland

In 2006, commissioning of the TransActinide Separator and Chemistry Apparatus TASCA [1], dedicated to investigate the chemical and physical properties of the heaviest elements, has started. One of TASCA's main foreseen applications is the use as a physical preseparator for chemical studies [2]. In this technique, EVaporation Residues (EVRs) are separated from the heavy-ion beam and from a significant fraction of unwanted byproducts of the nuclear reaction used to synthesize the element of interest. EVRs are extracted from the separator through a thin window. This separates TASCA's low-pressure region from the Recoil Transfer Chamber (RTC) in which EVRs are thermalized and made available for transport to a chemistry setup. This approach promises to allow significant progress in the chemical investigation of the heaviest elements as new techniques and new chemical compound classes become accessible for experimental study [2-4].

The RTC window that separates two different gas pressure regimes (~0.1-2 mbar inside TASCA, up to 2 bar in the RTC) has to meet the following requirements: i) He gas tightness at a pressure difference up to 2 bars, ii) small window thickness down to 100 µg/cm<sup>2</sup>. The first RTC prototype has been built in Berkeley [5] for chemical studies of Rf [3] produced in cold fusion reactions. The high Rf recoil energy has allowed using a 6-µm or a 3.3-µm thick Mylar foil on an aluminum support grid with 90% or 80% transparency, respectively. An RTC with a thinner Mylar window (2 µm) has been successfully tested at the gas filled separator GARIS (RIKEN, Japan) [6]. However, production of longer-lived, more neutron-rich transactinides requires using hot fusion reactions with actinide targets. The products of such reactions are so slow that their recoil ranges are very short. Therefore, more advanced, even thinner windows as well as appropriate support structures need to be developed.

TASCA features two ion-optical modes leading to different EVR images in the focal plane [7]: the High Transmission Mode (HTM) has maximum transmission but a relatively large image in the focal plane. About 80% of the transmitted EVRs of the "design reaction" <sup>48</sup>Ca+<sup>238</sup>U are deposited inside an area of ~(140x40) mm<sup>2</sup>. Reversing the polarity of the TASCA quadrupole magnets leads to the Small Image Mode (SIM) with a small image of ~(30x40) mm<sup>2</sup> at the cost of a somewhat reduced transmission. For reactions leading to relatively short-lived isotopes (T<sub>1/2</sub> ~s), the benefit of a small image size is expected to outweigh the loss in transmission.

The RTC window design is based on a standard Stainless Steel (SS) Conflat® flange with a nominal dia-

meter of 150 mm. The maximum size that can be accommodated by this flange has been chosen for the HTM and is (140x40) mm<sup>2</sup>. The window size for the SIM is only (30x40) mm<sup>2</sup>. The RTC window is supported by a honeycomb structure with 0.3 mm wide spokes and a hole pitch of 2.9 mm. It was made from hard SS by laser cutting. The outer grid dimensions are (144x44) mm<sup>2</sup> for the HTM and (34x44) mm<sup>2</sup> for SIM. The geometrical transmission is 80% (Figure 1a). To minimize losses due to non-parallel EVR trajectories, the grid has a thickness of only 1 mm. Because of the large working load on the large HTM window (up to ~100 kg), two bars were implemented in the flange to support the grid (Figure 1c). For ultra thin windows, a 20-µm thick Ni mesh with square (0.3x0.3) mm<sup>2</sup> holes and 20 µm wide spokes (Figure 1b) can be put on top of the metal grid. It has a transparency of 90% and was made by electro-etching. For aluminized Mylar foils with thicknesses of 1.5 µm or more, using the coarse grid only should be sufficient.

The windows for both, the HTM and the SIM, were successfully tested with Hg and Pb isotopes produced in <sup>40</sup>Ar induced reactions [8].

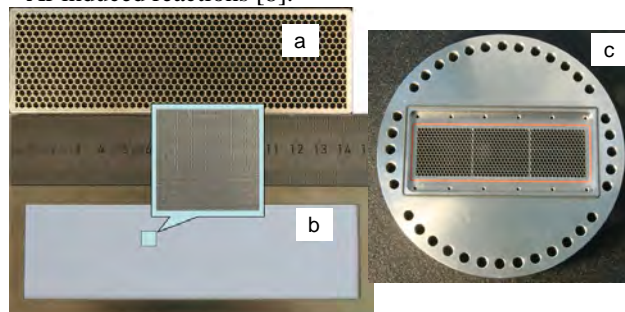


Figure 1: The honeycomb structure grid (a), the ultra fine Ni mesh (b) and the flange for the HTM (c).

### References

- [1] M. Schädel *et al.*, GSI Sci. Rep. 2005, Report 2006-1, 2006, p. 262; see also <http://www.gsi.de/TASCA>.
- [2] Ch.E. Düllmann *et al.*, Nucl. Instrum. Meth. A **551** (2005) 528.
- [3] J.P. Omtvedt *et al.*, J. Nucl. Radiochem. Sci. **3** (2002) 121.
- [4] R. Sudowe *et al.*, Radiochim. Acta **94** (2006) 123.
- [5] U.W. Kirbach *et al.*, Nucl. Instrum. Meth. A **484** (2002) 587.
- [6] H. Haba, contributions to TASCA workshops.
- [7] A. Semchenkov *et al.*, GSI Sci. Rep. 2004, Report 2005-1, p. 332.
- [8] Ch.E. Düllmann *et al.* contributions to this report.

\* alexander.yakushev@radiochemie.de

## Target Development for TASCA

K. Eberhardt<sup>1</sup>, J. V. Kratz<sup>1</sup>, D. Liebe<sup>1</sup>, P. Thörle<sup>1</sup>, W. Brühle<sup>2</sup>, Ch. E. Düllmann<sup>2</sup>, W. Hartmann<sup>2</sup>, A. Hübner<sup>2</sup>, E. Jäger<sup>2</sup>, B. Kindler<sup>2</sup>, B. Lommel<sup>2</sup>, M. Schädel<sup>2</sup>, B. Schausten<sup>2</sup>, E. Schimpf<sup>2</sup>, A. Semchenkov<sup>2,6</sup>, J. Steiner<sup>2</sup>, K. E. Gregorich<sup>3</sup>, H.-J. Maier<sup>4</sup>, J. Szerypo<sup>4</sup>, R. Sudowe<sup>5</sup>, A. Türler<sup>6</sup>, A. Yakushev<sup>6</sup>

<sup>1</sup>Johannes Gutenberg-Universität Mainz, Germany (UMZ); <sup>2</sup>GSI, Darmstadt, Germany; <sup>3</sup>Lawrence Berkeley National Laboratory, Berkeley, USA (LBNL); <sup>4</sup>Ludwigs-Maximilians-Universität München, Germany (LMU); <sup>5</sup>University of Nevada, Las Vegas, USA (UNLV); <sup>6</sup>Technische Universität München, Germany (TUM)

The main components of the TransActinide Separator and Chemistry Apparatus TASCA are already installed and the separator is now in the commissioning phase. A first beam time took place in April 2006 and further commissioning experiments were performed in May and November 2006. An overview of the current status is given in separate contributions [1-3].

In previous target tests, thin C- and Ti-foils proved to be more stable when irradiated with intense <sup>12</sup>C- and <sup>26</sup>Mg-beams compared to Al as a backing material. For the beam time in May a number of different targets materials have been applied, among them a set of <sup>nat</sup>Gd-targets produced by Molecular Plating at UMZ on a 5 µm Ti-backing foil. These targets have been irradiated with a 1.43 µA<sub>part</sub> Cr<sup>7+</sup>-beam. The targets withstood the irradiation without damage although the use of a relatively thick Ti-backing resulted in an increased background signal in the focal plane detectors. One main goal of the experiment in November was the test of different <sup>238</sup>U-targets with an intense <sup>40</sup>Ar-beam. Two target wheels have been irradiated – TN4 and TN8 – both consisting of three different kinds of targets. Table 1 comprises the target specifications. The number on the left indicate a particular segment.

Table 1: <sup>238</sup>U test-targets for TASCA

Target wheel TN4			
No.	Backing	Target	Cover
1	C, 40 µg/cm <sup>2</sup>	539 µg/cm <sup>2</sup>	C, 10 µg/cm <sup>2</sup>
2	Ti, 1.9 µm	521 µg/cm <sup>2</sup>	C, 10 µg/cm <sup>2</sup>
3	Ti, 1.9 µm	532 µg/cm <sup>2</sup>	not covered

Target wheel TN8			
No.	Backing	Target	Cover
1	C, 37 µg/cm <sup>2</sup>	539 µg/cm <sup>2</sup>	C, 10 µg/cm <sup>2</sup>
2	Ti, 2.2 µm	511 µg/cm <sup>2</sup>	C, 10 µg/cm <sup>2</sup>
3	Ti, 2.2 µm	491 µg/cm <sup>2</sup>	not covered

All targets have been delivered by the GSI target laboratory. Here, the U-layer has been produced by sputtering of depleted uranium in its metallic form with a <sup>235</sup>U content less than 0.2%. In some cases the target material has been covered with a thin C layer in order to prevent losses of the target material during irradiation with the <sup>40</sup>Ar<sup>7+</sup>-beam of successively increasing intensity. After a certain beam integral was applied, the targets have been inspected to

check for damage. Target wheel TN4 has first been irradiated for a total of 52'29" with increasing beam intensity up to 2 µA<sub>part</sub>. The target segments showed severe damage with holes and cracks. TN4 was then replaced by TN8 which was irradiated for 1h27'38" with increasing beam intensities up to 1 µA<sub>part</sub>. Figures 1 shows TN8 before and after irradiation, respectively. After irradiation segment 1 (C-backing) showed a visible whole, whereas segments 2 and 3 (Ti-backing) remained mechanically stable but show intense colour changes in the central part (see fig.1).



Figure 1: Target TN8 before (left) and after irradiation (right) with a <sup>40</sup>Ar-beam of 1 µA<sub>part</sub> maximum intensity.

Currently, the targets are further inspected by α-particle counting of the U-layer in order to check for material losses. Furthermore, the targets will be inspected by electron beam diagnostics and – if the activation products have decayed – by autoradiographic imaging [4] to check for losses and target homogeneity.

At UMZ work is currently under way to find optimum conditions for the deposition of <sup>244</sup>Pu (up to 500 µg/cm<sup>2</sup>) on 2 µm thin Ti backing foils by Molecular Plating from isobutanolic solution. <sup>244</sup>Pu is of special interest as a target material for chemical investigations of the heaviest elements, since relatively long lived isotopes of Rf to Hs – with half-lives in the order of a few seconds – can be produced in the bombardment of a <sup>244</sup>Pu-target with beams ranging from <sup>22</sup>Ne up to <sup>30</sup>Si. <sup>244</sup>Pu is also the optimum target for production of Z=114 with a <sup>48</sup>Ca beam.

## References

- [1] M. Schädel et al., contributions to this report
- [2] Ch. E. Düllmann et al., contributions to this report
- [3] A. Yakushev et al., contribution to this report
- [4] D. Liebe et al., contribution to this report

See also <http://www.gsi.de/TASCA>

## Improvements at the radiographic analysis of radioactive targets

D. Liebe<sup>1</sup>, K. Eberhardt<sup>1</sup>, J.V. Kratz<sup>1</sup>, W. Hartmann<sup>2</sup>, A. Huebner<sup>2</sup>, B. Kindler<sup>2</sup>, B. Lommel<sup>2</sup>, J. Steiner<sup>2</sup>

<sup>1</sup>Institut für Kernchemie, Johannes-Gutenberg-Universität Mainz (UMZ), Germany

<sup>2</sup>Gesellschaft für Schwerionenforschung, GSI, Darmstadt, Germany

Radiographic imaging (RI) is commonly used in life sciences to characterize radio labeled thin films, tissue sections, and electrophoresis gels. It can also provide information about the homogeneity and the thickness of radioactive targets on thin backings.

The newly available equipment at the institute for nuclear chemistry at UMZ is a FLA 7000 by FUJIFILM Corporation\*. This system is originally built as a multipurpose bio-imaging system for fluorescence dyes and medically relevant radioisotopes using reusable imaging plates (IP). The imaging plates are available for  $\beta$ - and  $\gamma$ -emitters, for weak  $\beta$ - and  $\alpha$ -emitters as well as for neutron detection.

The imaging plates consist of crystallites with sizes of 25  $\mu\text{m}$  or 50  $\mu\text{m}$ , depending on the IP. Each of the crystallites can be brought into an excited state by radiation and then analyzed by a 650 nm laser beam in the system. The experimental spatial resolution of the equipment has been determined by measuring a neutron activated gold wire with a thickness of 2.5  $\mu\text{m}$ . The achieved resolution for  $^{198}\text{Au}$  ( $E_{\beta} = 1.0 \text{ MeV}$ ,  $E_{\gamma} = 412 \text{ keV}$ ) was  $< 200 \mu\text{m}$ . With this, the resolution is improved by a factor of 10 compared to the formerly used autoradiographic imaging system [1]. The experimental resolution for uranium of the new equipment has not yet been determined. The imager is suitable for the direct determination of target thicknesses of actinide targets and for the investigation of their homogeneity.

In first investigations, the target thicknesses of thermally evaporated  $\text{UF}_4$  targets (made at GSI) have been verified by the imaging system and were compared to the thicknesses determined by a microbalance at GSI. Figure 1 shows the radiographic image of these targets.

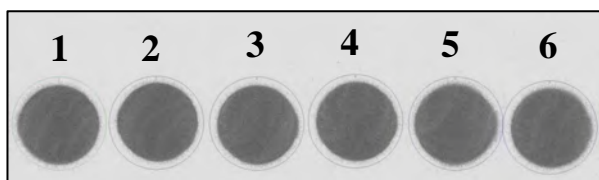


Figure 1: RI of the  $\text{UF}_4$  targets

The uranium contents in targets # 2-6 were determined relative to target # 1, which was used as "standard". The deviations range from 0.16 to 4.6 %, which is considered as good agreement, as listed in Table 1. From this, one can also conclude that there is no significant difference in the detection efficiency for the area covered by these six targets.

These results are in good agreement with an additional experiment investigating  $\alpha$ -decaying

\* in property of GSI

plutonium targets. Here, the content of two  $^{240}\text{Pu}$  samples with a known activity of 1.01 kBq and 0.087 kBq were determined and compared to each another.

Table 1: Thicknesses of the  $\text{UF}_4$ -targets determined by GSI and the FLA 7000 system

Target No	FLA 7000 [ $\mu\text{g}/\text{cm}^2$ ]	GSI [ $\mu\text{g}/\text{cm}^2$ ]	Deviation
1	„Standard“	389	0.00 %
2	376,4	377	0.16 %
3	360,3	364	1.02 %
4	363,4	369	1.53 %
5	363,3	381	4.64 %
6	364,9	372	1.90 %

In-depth studies with regard to the target thickness determination by the imaging system are still in progress. Especially, the preparation of standard actinide samples for a frequent use is under way.

Other investigations with the imaging system focus on its usability to survey the target layer homogeneity of uranium layers made by molecular plating. Here, the new system offers an improved resolution and better functional software compared to the formerly used equipment. Figure 2 shows the radiographic image of an uranium layer deposited on a tantalum backing.

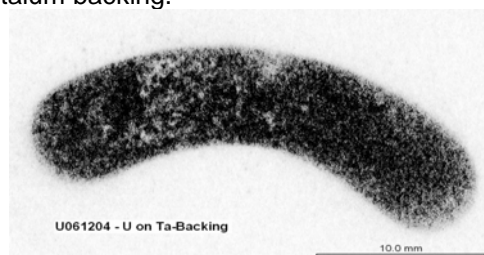


Figure 2: RI of an U-Target on Ta-Backing

The thickness of the U-layer is  $410 \mu\text{g}/\text{cm}^2$  as determined by neutron activation analysis. The deposition seems rather homogeneous in the right part of the target. Beginning from the middle towards the left, the layer in the image looks more inhomogeneous. The radiographic image confirms the inhomogeneity of the deposition of the target in reality. The central and the left part of the target have lost material and look furrowed, because the deposition layer was stressed when the target was dismantled from the deposition cell.

## References

[1] Liebe, D. et al, "The use of autoradiographic imaging for monitoring target thickness and homogeneity", Annual report, GSI, 2005

# Fast electrochemical deposition of Bismuth

H. Hummrich, J.V. Kratz

Institut für Kernchemie, Johannes Gutenberg-Universität Mainz, Germany

Fast electrochemical deposition is a promising method for the aqueous chemistry of the superheavy elements [1]. To perform electrodeposition experiments, the knowledge of basic electrochemical parameters like deposition potentials and the deposition velocity is necessary. To prepare experiments with element 115, its homolog Bi was investigated.

Experiments were performed with carrier free  $^{212}\text{Bi}$  ( $t_{1/2} = 60$  min,  $E_{\gamma} = 727$  keV). 1 ml of a solution of  $^{212}\text{Pb}$  in 0.5 M HCl was obtained via the emanation method [2]. The solution was passed through a column ( $d = 8$  mm,  $l = 15$  mm) filled with the cation exchanger Dowex 50x8 (100 - 200 mesh). Under the given conditions  $^{212}\text{Pb}$  is retained, whereas  $^{212}\text{Bi}$  forms an anionic chloro complex and passes the column. A total elution volume of 2 ml was sufficient to elute 90 % of the activity. The eluate was evaporated to dryness and dissolved in 1 ml 0.1 M HCl.

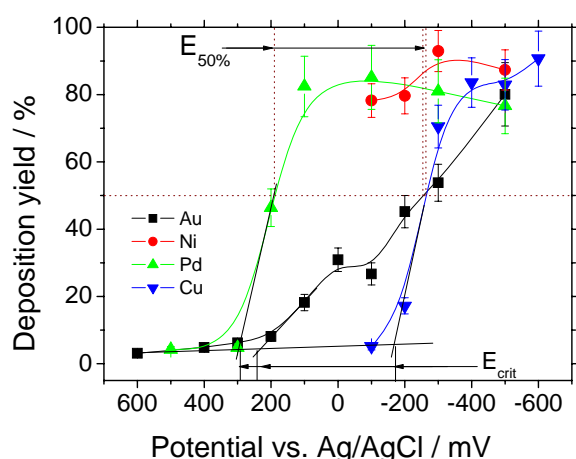


Figure 1: Potential curve for the electrochemical deposition of  $^{212}\text{Bi}$  on various electrodes from 0.1 M HCl.

Electrochemical deposition experiments were performed using a potentiostatic setup with an electrochemical cell for fast electrochemical depositions [3]. The electrolyte was 0.1 M HCl, the working electrode material was varied. 1 ml electrolyte containing  $^{212}\text{Bi}$  was electrolysed for 10 min, starting at the electrode rest potential which is obtained without applying external current. The deposited activity was measured for 1 min by  $\gamma$ -spectrometry and then electrolysis was resumed at a more negative potential etc.

Table 1:  $E_{\text{crit}}$  and  $E_{50\%}$  values for the deposition of Bi from 0.1 M HCl on various electrode materials

Electrode	$E_{\text{crit}}$	$E_{50\%}$
Au	+250	-240
Pd	+290	+180
Cu	-180	-260
Ni	spontaneous deposition	

Potential curves for the deposition of Bi on Au, Ni, Pd, and Cu are shown in Fig. 1. The critical potential ( $E_{\text{crit}}$ ), at which a significant deposition sets in, and the potential for the deposition of 50 % of the atoms in solution ( $E_{50\%}$ ), are indicated. Numbers are given in Table 1. In agreement with literature [4], a nearly complete deposition of Bi on Ni is already observed at the rest potential (spontaneous deposition). For the deposition on Cu and Pd, s-shaped curves are obtained. The corresponding  $E_{\text{crit}}$  and  $E_{50\%}$  values for the deposition on Pd and Cu differ more than 400 mV, meaning that the interaction of Bi and Pd is much stronger than the interaction of Bi with Cu. The deposition yield for the deposition on Au increases only slowly with decreasing potentials, resulting in a big difference in  $E_{\text{crit}}$  and  $E_{50\%}$ . This can be taken as a sign for a hindrance in the electrodeposition process.

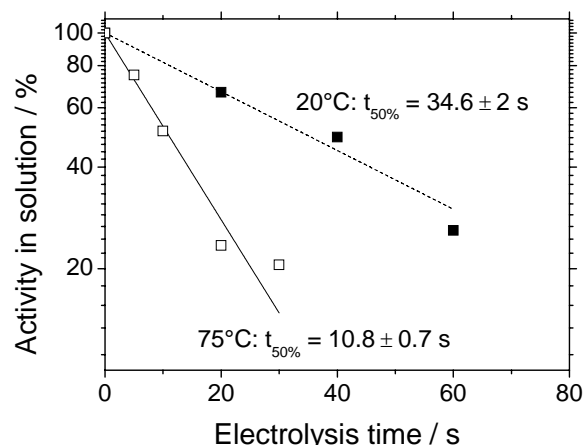


Figure 2: Electrodeposition velocity for the spontaneous electrodeposition of  $^{212}\text{Bi}$  on Ni from 0.1 M HCl at room temperature (filled squares) and at 75 °C (open squares).

The electrodeposition velocity was determined for the spontaneous deposition of  $^{212}\text{Bi}$  on Ni. Electrolysis was performed for a certain time and the deposited activity was measured. The time for the deposition of 50 % of the atoms in solution ( $t_{50\%}$ ) was 35 s at room temperature. This value could be lowered to 11 s by increasing the electrolyte temperature to 75 °C.

If isotopes of element 115 with a half-live in the range of 10 s were available, electrodeposition experiments should be performed with Ni or Pd electrodes.

## References

- [1] H. Hummrich et al., GSI Sci. Rep. 2005, p. 205
- [2] H. Hummrich et al., Jahresbericht des Instituts für Kernchemie, Uni Mainz 2002, A10
- [3] H. Hummrich et al., GSI Sci. Rep. 2004, p. 188
- [4] S.C. Ehinger, R.A. Pacer, F.L. Romines, J. Radioanal. Nucl. Chem. Articles 98, 39 (1986)